Mechanistic Insight into Size-Dependent Activity and Durability in Pt/CNT Catalyzed Hydrolytic Dehydrogenation of Ammonia Borane

9 AUTHORS, INCLUDING:

Xuezhi Duan
East China University of Science and Technology
51 PUBLICATIONS   277 CITATIONS

SEE PROFILE

Gang Qian
East China University of Science and Technology
47 PUBLICATIONS   303 CITATIONS

SEE PROFILE

De Chen
Norwegian University of Science and Technol…
237 PUBLICATIONS   4,798 CITATIONS

SEE PROFILE

Mechanistic Insight into Size-Dependent Activity and Durability in Pt/CNT Catalyzed Hydrolytic Dehydrogenation of Ammonia Borane

Wenyao Chen,[†] Jian Ji,[†] Xiang Feng,[†] Xuezhi Duan,*,[†] Gang Qian,[†] Ping Li,[†] Xinggui Zhou,[†] De Chen,*,[‡] and Weikang Yuan[†]

[†]State Key Laboratory of Chemical Engineering, East China University of Science and Technology, 130 Meilong Road, Shanghai 200237, China

[‡]Department of Chemical Engineering, Norwegian University of Science and Technology, Trondheim 7491, Norway

Ⓢ *Supporting Information*

ABSTRACT: We report a size-dependent activity in Pt/CNT catalyzed hydrolytic dehydrogenation of ammonia borane. Kinetic study and model calculations revealed that Pt(111) facet is the dominating catalytically active surface. There is an optimized Pt particle size of ca. 1.8 nm. Meanwhile, the catalyst durability was found to be highly sensitive to the Pt particle size. The smaller Pt particles appear to have lower durability, which could be related to more significant adsorption of B-containing species on Pt surfaces as well as easier changes in Pt particle size and shape. The insights reported here may pave the way for the rational design of highly active and durable Pt catalysts for hydrogen generation.

Downsizing metal particles to nanoscale in heterogeneous catalysis is often an effective method to boost the catalytic activity and thus achieve the high utilization of catalysts, which is the so-called size-dependent activity.[1] Such behavior in principle originates from the unique electronic and/or geometric properties,[2] and probing the dominating properties is highly desirable for rational design of catalysts. In addition to the activity, the kinetic behavior and durability of catalysts are also important factors. However, the size-dependence of such characteristics has not been addressed very much.

Pt is one of the most investigated and industrial relevant catalysts, and its superior catalytic performance has a strong dependence on the particle size.[3] The probe reaction in the present study is hydrolytic dehydrogenation of ammonia borane:

$$NH_3BH_3 + 2H_2O \rightarrow NH_4^+ + BO_2^- + 3H_2\uparrow$$
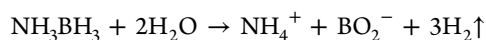
It has increasingly been attracted for hydrogen production at mild conditions for fuel cell applications.[4] Previous studies revealed that Pt catalysts, especially γ-Al_2O_3 or CNT supported small Pt nanoparticles and MIL-101 confined ones, showed much higher H_2 generation rate than other catalysts.[4,5] However, in these studies on Pt catalysis, both the size effects and support effects were simultaneously involved. In other words, the intrinsic size-dependent activity is still unclear, calling for fundamental understanding under keeping supports unchanged. Additionally, effects of Pt particle size on the kinetic behavior and durability have also not been reported previously. Therefore, an attempt would be made to explore the nature of the above effects

or behaviors and subsequently establish the structure−performance relationship.

In this work, we have employed the same close CNT support with the natures of highly crystalline and mesoporous[6] to load differently sized Pt nanoparticles. It makes it easy to be accessed by reactants, and it allows the imaging of almost all the particles for the accurate measurement of particle size distribution. On the resultant catalysts, intrinsic size-dependent H_2 generation activity has been investigated in hydrolytic dehydrogenation of ammonia borane. Subsequently, kinetic study and model calculations were further carried out to identify the dominating active sites as well as the contribution of the electronic and/or geometric effects to the activity. Moreover, the catalyst durability was also correlated to Pt particle size, and the possible deactivation mechanism was proposed.

Six differently sized Pt/CNT catalysts were prepared by only changing Pt loading without varying any other parameters that could affect the activity in which the procedure used has been previously reported.[5c] High angle annular dark field scanning transmission electron microscopy (HAADF-STEM) with high resolution was employed to characterize these catalysts for obtaining reliable particle size distributions.[7] Figures 1a and S1, Supporting Information (SI), show representative images of six Pt/CNT catalysts and the corresponding particle size distributions. The mean particle sizes were calculated based on the sizes of at least 200 random particles, and the results are summarized in Table S1, SI.

These catalysts were tested for hydrolytic dehydrogenation of ammonia borane in which the ratio of n_{Pt}/n_{AB} used for each reaction is maintained constant. The results of kinetic study are shown in Figure S2, SI. It is found that the accumulated hydrogen volume almost increases linearly with the reaction time in the initial period (e.g., AB conversion being in the range of 0−50%) for all the catalysts. It suggests a zero order reaction with respect to ammonia borane. Moreover, the observed zero order reaction suggests that the reaction is not limited by external diffusion of reactants in our kinetic studies. A first reaction order is expected for an external diffusion limited reaction. The external diffusion limitation free has also been confirmed by the results in Figure S3, SI, where the reaction rate is not influenced by the stirring speed. However, a deviation is from linear dependence of
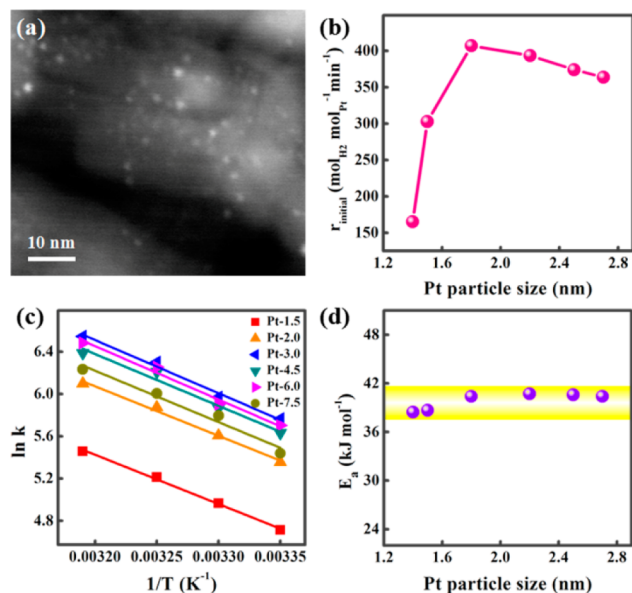
Figure 1. (a) Typical HAADF-STEM image of Pt/CNT with a Pt loading of 1.5 wt % (i.e., Pt-1.5). (b) Initial hydrogen generation rate ($r_{initial}$) as a function of Pt particle size. (c) ln k, derived from hydrogen generation rate versus reaction time, as a function of $1/T$ over differently sized Pt/CNT catalysts. (d) Activation energy as a function of Pt particle size.

accumulated hydrogen volume with the reaction time at the late stage of the reaction or high conversions of ammonia borane. It is possibly caused by the external diffusion limitation at low concentrations. As a result, the reaction rates can be easily determined based on the slope of the hydrogen generation curves in the initial reaction period in Figure S2, SI.

Initial rate ($r_{initial}$) of hydrogen generation over Pt/CNT catalysts was plotted as a function of the Pt particle size. As shown in Figure 1b, the $r_{initial}$ has a strong dependence on the mean Pt particle size (d_{Pt}), and the optimum one appears at d_{Pt} of 1.8 nm. The origin of this typical size-dependent activity would be revealed by combined kinetic study and model calculations as follows.

Considering that this reaction follows zero order kinetics over the above Pt/CNT catalysts in the initial period, the intrinsic activation energy (E_a) (SI) is easily derived by the observed overall hydrogen generation rate (i.e., the sum of the reaction rate of each type of active site) and expressed by

$$E_a = \frac{\sum_1^n A_i y_i \exp(-E_i/RT) E_i}{\sum_1^n A_i y_i \exp(-E_i/RT)} \tag{1}$$

where n is the number of the type of active site, and A_i, y_i and E_i are the pre-exponential factor, the fraction, and the activation energy of each type of active site, respectively.

On the basis of the results of kinetic experiments at 25−40 °C and the zero reaction order characteristic in the initial period (Figure S2, SI), reaction rate constant (k) was obtained from the slope of the fitting line. The logarithm of the as-obtained k was correlated to the reciprocal absolute temperature ($1/T$), and the results are shown in Figure 1c. Clearly, each Pt/CNT catalyst follows a good linearity between ln k and $1/T$. The corresponding slope of the plot yields E_a (Figure 1d). It is seen that all the E_a is in the range of 38−41 kJ/mol, which are not very sensitive to Pt particle size. By combining the almost unchanged E_a for differently sized Pt/CNT catalysts with eq 1, it could be

concluded that only one type of active site mostly contributes to the overall hydrogen generation rate. As a consequence, eq 1 can be simplified as

$$E_a = \frac{A_1 y_1 \exp(-E_1/RT) E_1}{A_1 y_1 \exp(-E_1/RT)} = E_1 \tag{2}$$

It is well-known that the change in the fraction of specific active sites (e.g., corner, edge, (111), or (100) site) with Pt particle size can be determined only when the particle shape is known. Previous studies showed that Pt nanoparticles of <5 nm in size are prone to exist as truncated octahedron.[8] They mainly consist of a mixture of (100) and (111) facets in order to minimize the total interfacial free energy. Herein, we employ high-resolution transmission electron microscopy (HRTEM) to characterize the Pt particle shape and find that CNT-supported Pt nanoparticles exhibit a well-defined shape in most cases. Figures 2a and S4, SI, show the representative shapes, which are
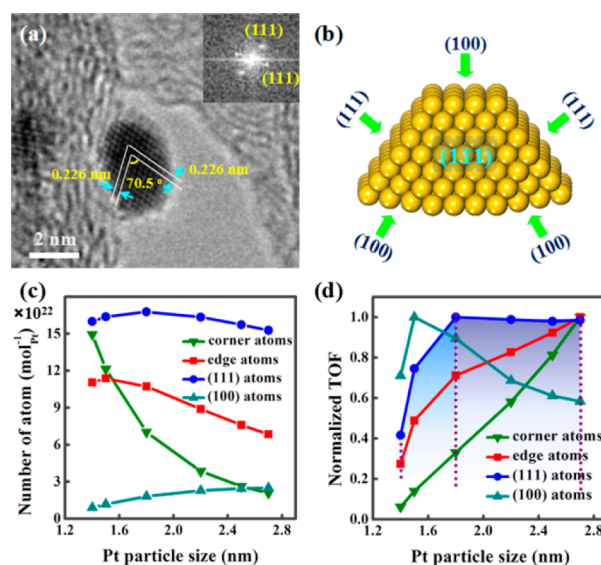
Figure 2. (a) Typical HRTEM image of Pt nanoparticle supported on CNT. (b) Schematic diagram of truncated cuboctahedron. (c) Plots of number of surface atoms per mole of Pt with Pt particle size of truncated cuboctahedron. (d) Plots of normalized TOF with Pt particle size.

best represented by the top slice of truncated cuboctahedron. To determine the type of the top facet of the above shape, the fast Fourier transform (FFT) of the selected area was further carried out. The top facet of (100) is observed, which is schematically shown in Figure 2b. The numbers of corner, edge, (111), and (100) atoms of each particle were calculated by formulas in Table S2, SI.[2c] The numbers of corner, edge, (111), or (100) atoms over differently sized Pt/CNT catalyst per mole of Pt were estimated by the number of corner, edge, (111), or (100) atoms of each particle times the number of particles. The results are shown in Figure 2c.

The activity of each specific type of active site was assumed to be uniform regardless of Pt particle size. If one type of Pt active site is responsible for the activity, the $r_{initial}$ of catalysts would increase linearly with the number of specific Pt active sites. Turnover frequency (TOF) of one type of active site, calculated from the data in Figures 1b and 2c, should be constant. Subsequently, each TOF point was normalized to the highest TOF for each type of active site to yield normalized TOF (SI). As shown in Figure 2d, the normalized TOF based on the number of

16737

dx.doi.org/10.1021/ja509778y | *J. Am. Chem. Soc.* 2014, 136, 16736−16739

corner or edge sites increases monotonically with increasing Pt particle size, respectively. The normalized TOF based on the number of the sites on (100) facet appears volcano-shaped as a function of Pt particle size. However, only when (111) facet atoms are considered as active sites, the normalized TOF is almost constant for Pt particles with the size of ≥1.8 nm. It is suggested that the (111) facets of Pt/CNT catalysts are dominating active sites for hydrolytic dehydrogenation of ammonia borane. Moreover, as shown in Figure 2c, the number of Pt(111) atoms of differently sized Pt/CNT catalyst follows a volcano curve with Pt particle size, i.e., 1.8 nm sized Pt/CNT catalyst has the maximum. This could be one reason for the volcano relationship between $r_{initial}$ and Pt particle size (Figure 1b).
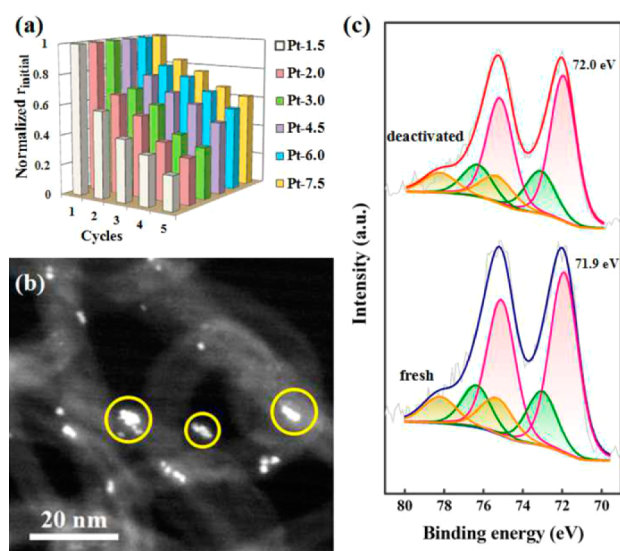
However, it can be also seen that on the smaller sized Pt/CNT catalysts (i.e., the particle size of <1.8 nm) the normalized TOF increases monotonically with increasing Pt particle size (Figure 2d). This may be dominated by electronic properties rather than geometric properties.[2a] The above results not only unravel the origin of the size-dependent activity but also reveal 1.8 nm sized Pt/CNT catalyst being optimum with the highest catalytic activity and utilization of Pt. This might guide the rational design of highly active Pt catalysts.

Beside the activity and kinetic behavior measurements, the durability evaluation of catalysts is also an important issue.[9] The durability of differently sized Pt/CNT catalysts was evaluated to explore the effects of the Pt particle size on the durability. To this end, the recyclability of each catalyst was evaluated up to 5 cycles (Figure S5, SI), where the new ammonia borane aqueous solution was added into the reactor after the completion of the last run. The deactivation function, which is defined as the $r_{initial}$ in each cycle (Figure S5, SI) normalized by the $r_{initial}$ in the first cycle, is presented in Figure 3a as a function of cycle number and Pt particle size. The gradual decreases in the catalytic activity are observed for all the catalysts. The results in Figure 3a clearly indicate a size-dependent durability. In particular, the smaller the Pt particle size, the faster the deactivation. For example, the smallest sized Pt/CNT catalyst (i.e., 1.4 nm) suffers from a severe

deactivation, and its activity in the fifth cycle is ca. 24% of its initial activity. It is worth to mention that the AB concentration decreases with the cycle number due to the accumulation of water. However, both the molar ratio of Pt to AB and the amount of catalyst are kept constant in each cycle. Then, effects of AB concentration on the hydrogen generation rate were further studied, and the typical results are shown in Figure S6, SI. It was found that the $r_{initial}$ is almost independent of the AB concentration. The results suggest that the observed decrease in the activity with the cycle number (Figure 3a) should be a result of catalyst deactivation.

Taking Pt/CNT catalyst with the 1.4 nm of Pt particle size and the lowest durability, for example, the difference in the geometric and electronic properties between fresh catalyst and deactivated catalyst after 5 cycles was probed to gain insights into the deactivation mechanism of the catalysts. The deactivation mechanisms of pore blocking and metal leaching can be first ruled out because mesoporous close-CNT was used and no platinum species in filtrate were detected, respectively. The deactivated catalyst was characterized by HAADF-STEM. Results in Figure 3b show that the deactivated catalyst contains some agglomerated Pt particles with irregular shape in comparison to the fresh catalyst (Figure 1a). However, the used Pt-7.5 catalyst after 5 cycles (Figure S7, SI) shows similar Pt particle size distribution compared to the fresh Pt-7.5 catalyst. This may be a result of that the smaller particles have higher surface energy and thus tend to aggregate into larger particles during the reaction. Therefore, the more significant agglomeration of the smaller sized Pt particles could be one reason for the lower durability.

Inspired by previous studies on the deactivation mechanism of NaBH$_4$ hydrolysis (i.e., strongly adsorbed B-containing species coating metal active sites),[10] we further studied whether B-containing species could strongly adsorb on the surfaces of Pt nanoparticles and thus lead to the deactivation of the catalyst. The deactivated Pt-1.5 catalyst after 5 cycles was washed using distilled water until not detecting B-containing species in the filtrate by ICP. The washed Pt-1.5 catalyst was characterized by ICP and CO chemisorption and compared to the fresh one. The results are shown in Table 1.

Table 1. Relative Content of Pt Species, Pt Dispersion, and B Content of the Fresh and Deactivated Pt-1.5 Catalysts

catalyst	relative content (%)			B content (wt %)[a]	Pt dispersion (%)[b]
	Pt^0	Pt^{2+}	Pt^{4+}		
fresh	64	21	15	0	72
deactivated	63	22	15	0.2	10

[a]Measured by ICP. [b]Measured by CO chemisorption.

Inductively coupled plasma (ICP) measurements show that the washed deactivated Pt-1.5 catalyst has the 0.2 wt % of the B content. CO chemisorption measurements show that the Pt dispersion of the deactivated catalyst is 10%, which is much lower than that of the fresh catalyst (72%). The estimated Pt particle size based on the measured Pt dispersion of the deactivated catalyst is ca. 11.3 nm. It is much larger than that observed by HAADF-STEM (Figure 3b). It suggests that strong adsorption of B-containing species on the Pt surfaces could be another reason for the catalyst deactivation. In addition, it is reasonable to assume that the larger fraction of Pt surfaces with low coordination number on smaller Pt particles could result in a

Figure 3. (a) Relative activities over cycles of Pt catalysts with different Pt loadings for the hydrolysis of ammonia borane. (b) Typical HAADF-STEM image of deactivated Pt-1.5 catalyst after 5 cycles. (c) XPS spectra of fresh Pt-1.5 catalyst and deactivated Pt-1.5 catalyst after 5 cycles.

16738

dx.doi.org/10.1021/ja509778y | J. Am. Chem. Soc. 2014, 136, 16736−16739

more significant adsorption of B-containing species during the reaction. This may be the main cause for the severe deactivation of the smaller sized Pt/CNT catalyst.

Subsequently, X-ray photoelectron spectroscopy (XPS) was further employed to probe the difference in the electronic properties between fresh and deactivated Pt-1.5 catalysts. Figure 3c shows the Pt 4f XPS spectra of fresh and deactivated catalysts, and Table 1 shows the relative contents of Pt^0, Pt^{2+}, and Pt^{4+} from the deconvolution analyses. It is observed that both catalysts have similar Pt^0, Pt^{2+}, and Pt^{4+} contents, that is, 64, 21, and 15% for the fresh catalyst, while 63, 22, and 15% for the deactivated catalyst. Moreover, the binding energy of metallic Pt $4f_{7/2}$ for the deactivated catalyst is 72.0 eV, which is slightly higher than that for the fresh catalyst (71.9 eV). This could be due to the adsorption of B-containing species with higher electronegative properties creating more oxidized environment.[11] In our previous work, we have observed that the positive shift of Pt $4f_{7/2}$ binding energy led to an increase in the hydrogen generation rate.[5c] Therefore, the observed catalyst deactivation cannot be ascribed to the electronic modification of Pt/CNT catalyst.

In summary, we identify experimentally and theoretically that Pt(111) is a dominating catalytically active surface, and ca. 1.8 nm sized Pt/CNT catalyst is optimum with the highest catalytic activity and utilization of Pt. Moreover, the smaller the Pt particle size, the lower the durability. The plausible mechanism of size-dependent durability has been proposed by using multiple techniques such as HAADF-STEM, XPS, ICP, and CO chemisorption. Strongly adsorbed B-containing species and the change in the Pt particle size and shape are the two main causes for the catalyst deactivation. These results demonstrate that Pt particle size plays a crucial role in the design and optimization of active and durable catalysts for hydrolytic dehydrogenation of ammonia borane.

■ ASSOCIATED CONTENT

Ⓢ Supporting Information

Experimental procedures, kinetic formulas derivation, normalized TOF derivation, Tables S1 and S2, and Figures S1–S7. This material is available free of charge via the Internet at http://pubs.acs.org.

■ AUTHOR INFORMATION

Corresponding Authors
*xzduan@ecust.edu.cn
*chen@nt.ntnu.no

Notes
The authors declare no competing financial interest.

■ ACKNOWLEDGMENTS

■ REFERENCES

(1) (a) Bell, A. T. *Science* **2003**, *299*, 1688. (b) Mizuno, N.; Misono, M. *Chem. Rev.* **1998**, *98*, 199. (c) Chen, M. S.; Cai, Y.; Yan, Z.; Gath, K. K.; Axnanda, S.; Goodman, D. W. *Surf. Sci.* **2007**, *601*, 5326. (d) Polshettiwar, V.; Varma, R. S. *Green Chem.* **2010**, *12*, 743. (e) Li, Y.; Somorjai, G. A. *Nano Lett.* **2010**, *10*, 2289. (f) Sanchez, A.; Abbet, S.; Heiz, U.; Schneider, W. D.; Hakkinen, H.; Barnett, R. N.; Landman, U. *J. Phys. Chem. A* **1999**, *103*, 9573.

(2) (a) Wilson, O. M.; Knecht, M. R.; Garcia-Martinez, J. C.; Crooks, R. M. *J. Am. Chem. Soc.* **2006**, *128*, 4510. (b) Mayrhofer, K. J. J.; Blizanac, B. B.; Arenz, M.; Stamenkovic, V. R.; Ross, P. N.; Markovic, N. M. *J. Phys. Chem. B* **2005**, *109*, 14433. (c) Van Hardeveld, R.; Hartog, F. *Surf. Sci.* **1969**, *15*, 189. (d) Bond, G. C. *Surf. Sci.* **1985**, *156*, 966. (e) Den Breejen, J. P.; Radstake, P. B.; Bezemer, G. L.; Bitter, J. H.; Froseth, V.; Holmen, A.; De Jong, K. P. *J. Am. Chem. Soc.* **2009**, *131*, 7197.

(3) (a) Van Santen, R. A. *Acc. Chem. Res.* **2009**, *42*, 57. (b) Kuhn, J. N.; Huang, W.; Tsung, C. K.; Zhang, Y.; Somorjai, G. A. *J. Am. Chem. Soc.* **2008**, *130*, 14026. (c) Tsung, C. K.; Kuhn, J. N.; Huang, W. Y.; Aliaga, C.; Hung, L. I.; Somorjai, G. A.; Yang, P. D. *J. Am. Chem. Soc.* **2009**, *131*, 5816. (d) Arenz, M.; Mayrhofer, K. J. J.; Stamenkovic, V.; Blizanac, B. B.; Tomoyuki, T.; Ross, P. N.; Markovic, N. M. *J. Am. Chem. Soc.* **2005**, *127*, 6819. (e) Allian, A. D.; Takanabe, K.; Fujdala, K. L.; Hao, X.; Truex, T. J.; Cai, J.; Buda, C.; Neurock, M.; Iglesia, E. *J. Am. Chem. Soc.* **2011**, *133*, 4498. (f) Chin, Y. H.; Buda, C.; Neurock, M.; Iglesia, E. *J. Am. Chem. Soc.* **2011**, *133*, 15958. (g) Plomp, A. J.; Vuori, H.; Krause, A. O.; De Jong, K. P.; Britter, J. H. *Appl. Catal., A* **2008**, *351*, 9.

(4) (a) Staubitz, A.; Robertson, A. P. M.; Manners, I. *Chem. Rev.* **2010**, *110*, 4079. (b) Jiang, H. L.; Singh, S. K.; Yan, J. M.; Zhang, X. B.; Xu, Q. *ChemSusChem* **2010**, *3*, 541. (c) Yadav, M.; Xu, Q. *Energy Environ. Sci.* **2012**, *5*, 9698. (d) Demirci, U. B.; Miele, P. *Energy Environ. Sci.* **2009**, *2*, 627. (e) Yan, J. M.; Zhang, X. B.; Akita, T.; Haruta, M.; Xu, Q. *J. Am. Chem. Soc.* **2010**, *132*, 5326. (f) Metin, O.; Mazumder, V.; Ozkar, S.; Sun, S. *J. Am. Chem. Soc.* **2010**, *132*, 1468.

(5) (a) Chandra, M.; Xu, Q. *J. Power Sources* **2006**, *156*, 190. (b) Chandra, M.; Xu, Q. *J. Power Sources* **2007**, *168*, 135. (c) Chen, W. Y.; Ji, J.; Duan, X. Z.; Qian, G.; Li, P.; Zhou, X. G.; Chen, D.; Yuan, W. K. *Chem. Commun.* **2014**, *50*, 2142. (d) Aijaz, A.; Karkamkar, A.; Choi, Y. J.; Tsumori, N.; Ronnebro, E.; Autrey, T.; Shioyama, H.; Xu, Q. *J. Am. Chem. Soc.* **2012**, *134*, 13926. (e) Wang, X.; Liu, D. P.; Song, S. Y.; Zhang, H. J. *Chem. Commun.* **2012**, *48*, 10207.

(6) (a) Zhu, J.; Holmen, A.; Chen, D. *ChemCatChem* **2013**, *5*, 378. (b) Serp, P.; Corrias, M.; Kalck, P. *Appl. Catal., A* **2003**, *253*, 337.

(7) Zhang, B.; Zhang, W.; Su, D. S. *ChemCatChem* **2011**, *3*, 965.

(8) (a) Lim, B.; Jiang, M. J.; Camargo, P. H. C.; Cho, E. C.; Tao, J.; Lu, X. M.; Zhu, Y. M.; Xia, Y. N. *Science* **2009**, *324*, 1302. (b) Wang, C.; Daimon, H.; Onodera, T.; Koda, T.; Sun, S. *Angew. Chem., Int. Ed.* **2008**, *47*, 3588.

(9) (a) Bartholomew, C. H. *Appl. Catal., A* **2001**, *212*, 17. (b) Baylet, A.; Royer, S.; Marecot, P.; Tatibouet, J. M.; Duprez, D. *Appl. Catal., B* **2008**, *77*, 237. (c) Li, Y. M.; Liu, J. H. C.; Witham, C. A.; Huang, W. Y.; Marcus, M. A.; Fakra, S. C.; Alayoglu, P.; Zhu, Z. W.; Thompson, C. M.; Arjun, A.; Lee, K.; Gross, E.; Toste, F. D.; Somorjai, G. A. *J. Am. Chem. Soc.* **2011**, *133*, 13527.

(10) Akdim, O.; Demirci, U. B.; Miele, P. *Int. J. Hydrogen Energy* **2011**, *36*, 13669.

(11) (a) Montilla, F.; Morallon, E.; De Battisti, A.; Barison, S.; Daolio, S.; Vazquez, J. L. *J. Phys. Chem. B* **2004**, *108*, 15976. (b) Park, H.; Kim, Y. K.; Choi, W. *J. Phys. Chem. C* **2011**, *115*, 6141.